

Flood Capacity of Shirakawa River at Tatsudajinnai Area in Kumamoto Prefecture

Xiang Chen^{1,*}, Ryuichi Hirakawa², Terunori Ohmoto³

¹Environment and Life Engineering, Graduate School of Engineering, Maebashi Institute of Technology, Maebashi, Japan

²Department of Civil and Environment Engineering, Maebashi Institute of Technology, Maebashi, Japan

³Faculty of Advanced Science and Technology, Kumamoto University, Kumamoto, Japan

Email address:

m1646502@maebashi-it.ac.jp (Xiang Chen), hirakawa@maebashi-it.ac.jp (R. Hirakawa), ohmoto@kumamoto-u.ac.jp (T. Ohmoto)

*Corresponding author

To cite this article:

Xiang Chen, Ryuichi Hirakawa, Terunori Ohmoto. Flood Capacity of Shirakawa River at Tatsudajinnai Area in Kumamoto Prefecture. *International Journal of Economy, Energy and Environment*. Vol. 3, No. 5, 2018, pp. 51-57. doi: 10.11648/j.ijeee.20180305.13

Received: November 13, 2018; **Accepted:** December 10, 2018; **Published:** December 27, 2018

Abstract: In the Shirakawa River, remarkable deformation due to sediment deposition was observed after the river channel improvement work. The sediment deposition was observed at the bend of the river channel. In this research, a model experiment, a quasi-three-dimensional numerical simulation and planer two-dimensional bed variation analysis were conducted in order to evaluate the effect of river bend curvature variation caused by improvement works on channel response and flow capacity. In the model experiment, large sandbars were formed, and the channel become narrower. In the numerical simulation, flood flew over sandbars and gravel deposited on sandbars, which caused decreasing of flow capacity. The gravel deposition was most active when the flow charge was in its peak. There was less inundation at the areas where sediment deposition was occurred.

Keywords: Flood Disaster, Deposition, Topographical Changes, Hydraulic Model Experiment, Quasi-3D Flood Flow Model, Shirakawa River

1. Introduction

In disaster restoration, it is important to establish a disaster prevention system. However, there were many cases that an area was damaged by floods frequently [1]. One of the reasons is that the disaster restoration was carried out without sufficient consideration of river channel characteristics.

The Shirakawa River (a class-A river), which flows through Kumamoto prefecture, is one of the river which floods often occurs. From July 11 to 13, 2012, heavy rain hit northern part of Kyushu due to the stagnation of the Baiu front [2-4]. The flow discharge was 2300m³/s, which was much larger than the flood capacity. Highest water level was also recorded at the Yotsugi Bridge (12.3km from river mouth of the Shirakawa River). The Shirakawa River overflowed due to this heavy rain, and some areas in Kumamoto City were seriously damaged by the flood (Figure 1).

After this flood, an improvement work to reduce the

sinuosity of the Shirakawa River was carried out. This work took 5 years, and the Shirakawa River switched to the new channel (Figure 2) in July 2017.

On the other hand, the shape of the river channel gradually changes with time. There was a previous research about the environment and channel property of a river after improvement work (the Kitagawa River at Miyazaki prefecture) [5-8].

In case of the Shirakawa River, about 200m long sediment accumulation was occurred on the inner side of the bend of the new channel by the flood after the improvement work (Figure 3). In disaster management, it is very important to consider about the river morphology change and flood capacity.

In this research, a model experiment and quasi-3D numerical analysis was conducted in order to simulate the river morphology change by a flood, and the effect of the river morphology on flood capacity.



Figure 1. Flood of July 2012 at the Shirakawa River.



Figure 2. New channel of the Shirakawa River.



Figure 3. Sediment accumulation at the Shirakawa River.

2. New Channel of the Shirakawa River

The average riverbed gradient of the new channel is 1/700 at the straight part and 1/10 at the bend. The average width of the new channel is 100m at the straight part and 160m at the bend. In order to prevent riverbed erosion, the riverbed was paved with stones of more than 200cm large.

After the improvement work, floods (about 1500m³/s)

often occurred to the Shirakawa River. Moreover, a large earthquake hit the area near the Shirakawa River in April 2017. Because of these floods and the earthquake, a large amount of sediment flowed in the new channel.

3. Hydraulic Model Experiment

The hydraulic model experiment was conducted in order to evaluate the effect of sediment accumulation on floods and channel morphology. The target area of the model experiment was 18.5km ~ 19.6km section from the river mouth. The scale of the hydraulic model was set to 1/100 scale according to Froude number similarity (Figure 4). The Froude number of the hydraulic model was set to the same value with the actual Shirakawa River. Table 1 is the scale ratio of parameters. In order to eliminate the effect of surface tension, the model was moistened before the experiment.

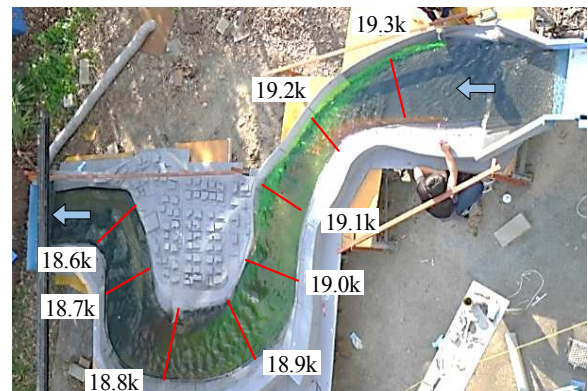


Figure 4. Hydraulic model.

The Manning's roughness coefficient of the channel bed was 0.034m^{-1/3}s. The corresponding Manning's roughness coefficient in the model was 0.016 m^{-1/3}s. The Manning's roughness coefficient in the model was controlled by paving sand (median particle size = 5mm) on the channel bed of the model. The model was assumed to be no erosion.

4. Flow Analysis

For the quasi-3D flood flow analysis model [9-12], a quasi-three-dimensional model based on the solution of three-dimensional incompressible Reynolds averaged Navier-Stokes equation with the assumption of Boussinesq approximation and hydrostatic pressure was used. The continuity equation and the equation of motion used for calculation are shown below. For the calculation, the formula was differentiated using the finite volume method.

Table 1. Scale ratio of parameters.

Fundamental quantity	Dimension	Reduction	Scale
Length, Depth (h)	L	S	1/100
Discharge (Q)	L ³ ·T ⁻¹	S ^{5/2}	1/100,000
Velocity (V)	L·T ⁻¹	S ^{1/2}	1/10
Time (T)	T	S ^{1/2}	1/10
Resistance coefficient (n)	L ^{-1/3} ·T	S ^{1/6}	1/2.15

$$\frac{\partial U}{\partial t} + \frac{\partial F_x^I}{\partial x'} + \frac{\partial F_y^I}{\partial y'} + \frac{\partial F_\sigma^I}{\partial \sigma} + \frac{\partial F_x^V}{\partial x} + \frac{\partial F_y^V}{\partial y} + \frac{\partial F_\sigma^V}{\partial \sigma} = S \quad (1)$$

$$U = \begin{bmatrix} h \\ hu \\ hv \end{bmatrix}$$

$$F_x^I = \begin{bmatrix} h\bar{u} \\ hu^2 + \frac{1}{2}g(h^2 - d^2)h\bar{u} \\ huv \end{bmatrix}$$

$$F_x^V = \begin{bmatrix} 0 \\ hA \left(2 \frac{\partial u}{\partial x} \right) \\ hA \left(\frac{\partial u}{\partial y} + \frac{\partial v}{\partial x} \right) \end{bmatrix}$$

$$F_y^I = \begin{bmatrix} h\bar{v} \\ hvu \\ hv^2 + \frac{1}{2}g(h^2 - d^2) \end{bmatrix} \quad (2)$$

$$F_y^V = \begin{bmatrix} 0 \\ hA \left(\frac{\partial u}{\partial y} + \frac{\partial v}{\partial x} \right) \\ hA \left(2 \frac{\partial v}{\partial x} \right) \end{bmatrix}$$

$$F_\sigma^I = \begin{bmatrix} h\omega \\ h\omega u \\ h\omega v \end{bmatrix}$$

$$F_\sigma^V = \begin{bmatrix} 0 \\ \frac{v_t}{h} \frac{\partial u}{\partial \sigma} \\ \frac{v_t}{h} \frac{\partial v}{\partial \sigma} \end{bmatrix}$$

$$S = \begin{bmatrix} 0 \\ g\eta \frac{\partial d}{\partial x} - \frac{h}{\rho_0} \frac{\partial p_a}{\partial x'} \\ g\eta \frac{\partial d}{\partial y} - \frac{h}{\rho_0} \frac{\partial p_a}{\partial y'} \end{bmatrix}$$

Where I is the inviscid flux, V is the viscous flux, t is time. x, y and z are Cartesian coordinates. η is water level. d is water depth, $h = \eta + d$ is total water depth. u, v are flow velocity of x, y direction. g is gravitational acceleration. v_t is vertical (or eddy) turbulence viscosity. p_a is atmosphere pressure. ρ_0 is water density.

Table 2. Calculation condition.

Parameters	Value	Unit
Mesh		
River way (stream×transversal)	20×10	m
Simulation time	7200	sec
Time step	0.2	sec
Bed resistance	0.031	m ^{-1/3} s
Discharge	2300	m ³ /s

In order to verify the validity of the flow analysis model, the water level and flow velocity acquired by model experiment and numerical simulation were compared. The calculation conditions are shown in Table 2. Figure 5 shows the comparison of the numerical analysis value and the water surface profile in the vertical direction of the river channel measured by the point gauge in the model experiment. Both water levels are well matched, except the right side of 19.0km ~ 19.1km section, and the left side of 18.6km ~ 18.7km section

Figure 6 shows the surface flow velocity vector at the flood discharge of 2300m³/s by the model experiment using Particle Image Velocimetry (PIV). Figure 7 shows the surface flow velocity distribution by numerical simulation. As a result, similar results were obtained by the model experiment and the numerical simulation. The maximum velocity reached to 7.5m/s.

Figure 8 shows the comparison of the measured value and calculated value of flow velocity distribution at the riverbed. The actual value was measured at the height of 1cm from the bottom of the riverbed by the electromagnetic current meter. The measured value and calculated value were almost same at most of areas except at the bend at the 18.6km ~ 18.7km section, and the 19.0km point which the flow attacks the right bank.

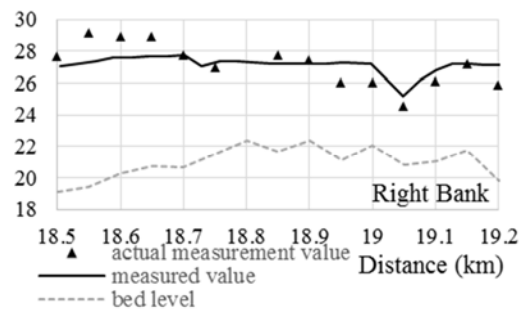
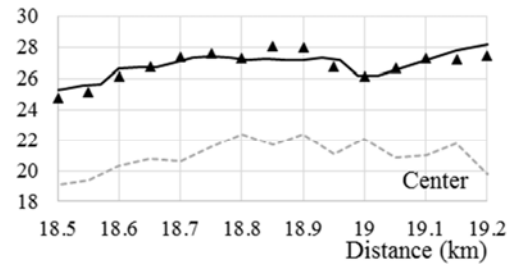
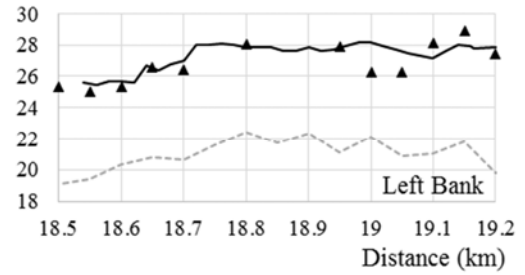


Figure 5. Comparison of the numerical analysis value and the measured value of the water surface profile in the vertical direction of the river channel.

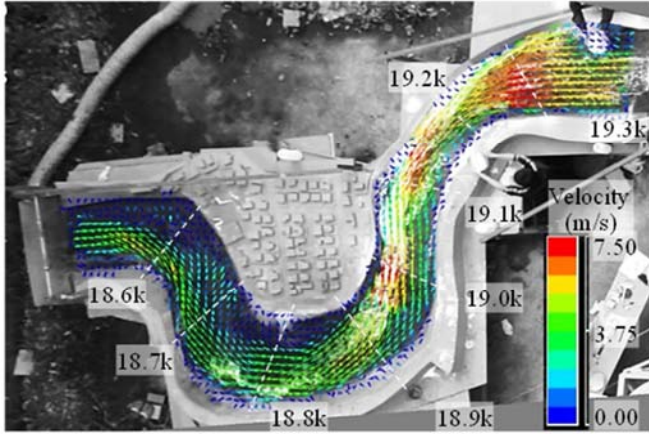


Figure 6. Surface flow velocity vectors at the flood discharge of 2300m³/s measured by PIV.

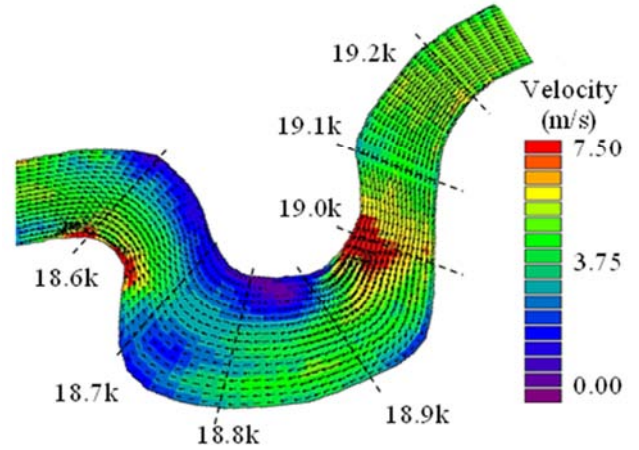


Figure 7. Surface flow velocity distribution by numerical simulation.

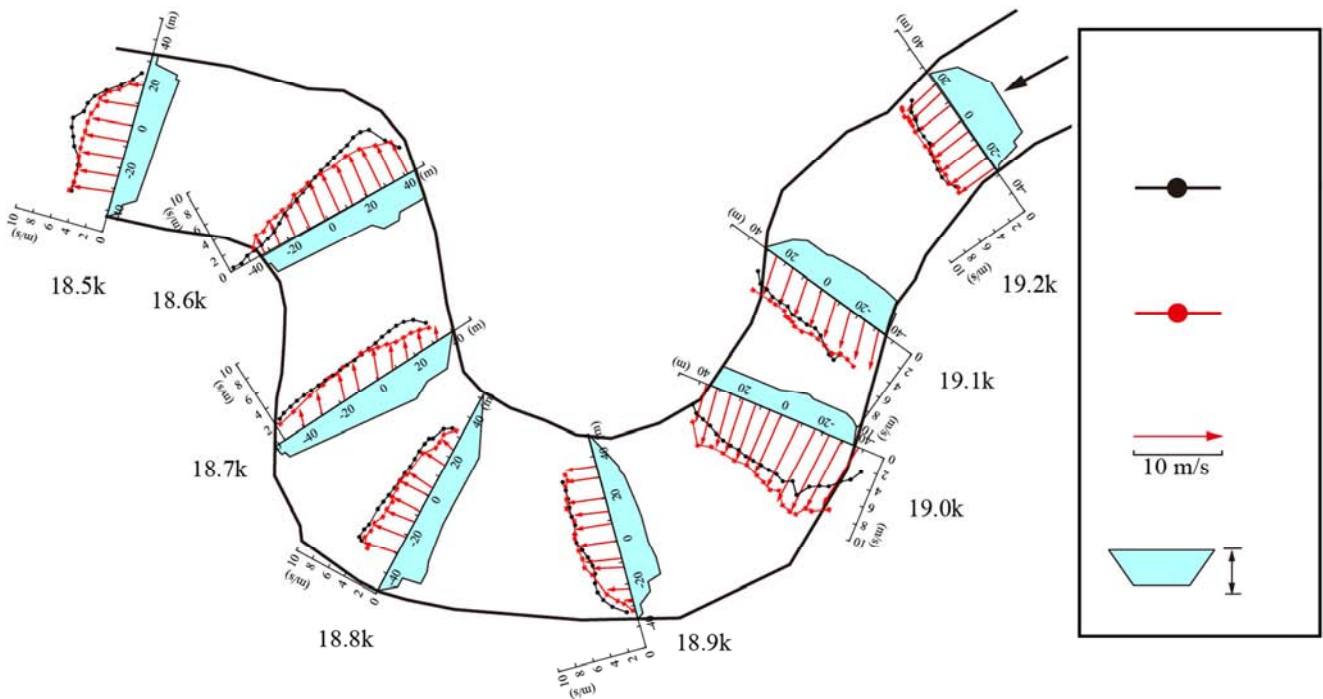


Figure 8. Comparison of the measured value and calculated value of flow velocity distribution at the riverbed.

5. Response Characteristics of River Channels

5.1. Analysis Method

Two-dimensional riverbed variation analysis was conducted in order to evaluate the effect of riverbed morphology variation on the flood capacity. The sediment discharge was calculated using Meyer-Peter and Müller formula [13]. The continuous equation of sediment transport is;

$$-(1 - n) \frac{\partial z}{\partial t} = \frac{\partial S_x}{\partial x} + \frac{\partial S_y}{\partial y} \quad (3)$$

where z is riverbed height. n is the porosity of sediment of the river bed. t is time. S_x , S_y are sediment discharge per unit width of x , y direction. The sediment discharge per unit width can be calculated by following equation;

$$S_{bl} = 8(\theta' - \theta_c)^{1.5} \sqrt{(s - 1)gd_{50}^3} \quad (4)$$

$$S_x = S_{bl} \times \cos \phi \quad (5)$$

$$S_y = S_{bl} \times \sin \phi \quad (6)$$

Where $\phi = \tan^{-1}(u_b/v_b)$, u_b , v_b are flow velocity of x , y direction at riverbed. θ' is dimensionless tractive force. θ_c is critical tractive force.

5.2. Verification of Analysis Model

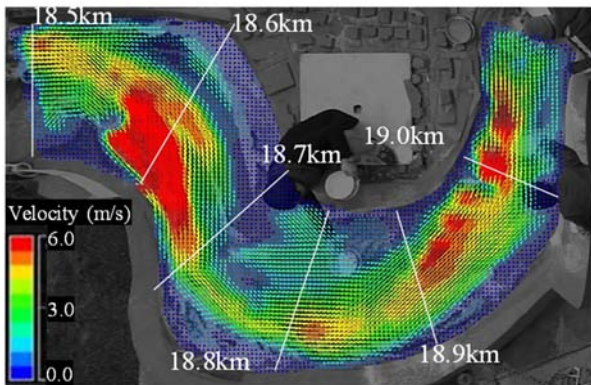


Figure 9. Surface flow velocity by hydraulic model experiment.

In order to verify the validity of the riverbed variation analysis model, the riverbed variation by a flood of 2000m³/s in the model experiment was reproduced. In the hydraulic model experiment, water (flow rate = 2.0L/s) and sand (particle diameter $d_{50} = 1.7\text{mm}$) were fed for 2 hours. Figure 9 shows the surface flow velocity distribution 2 hours later under the above conditions. The channel of 18.8km ~ 19.0km became narrow due to sediment accumulation, and the flow

velocity at the point of 19.0km become faster (5~6m/s). Figure 10 shows the flow velocity distribution by numerical simulation. Similar result was obtained for the hydraulic model experiment and the numerical simulation. Figure 11 shows the measured value and calculated value of the thickness of the sediment accumulation. Similar result was obtained for the hydraulic model experiment and the numerical simulation.

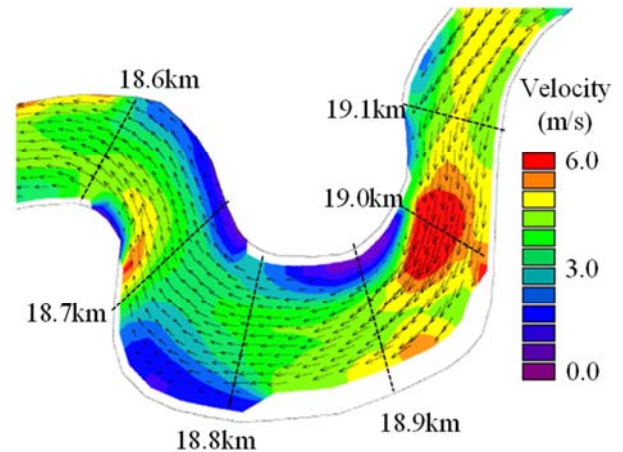


Figure 10. Flow velocity distribution by numerical simulation.

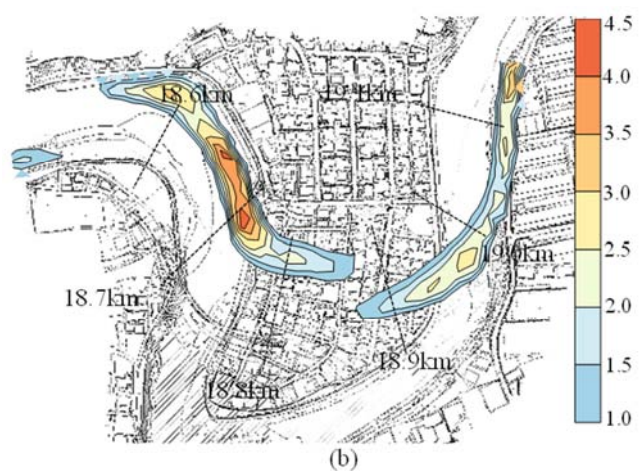
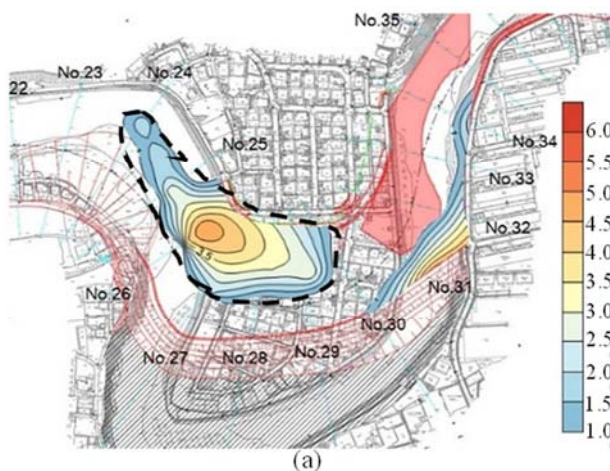


Figure 11. Measured value (upper Figure) and calculated value (lower Figure) of the thickness of the sediment accumulation.

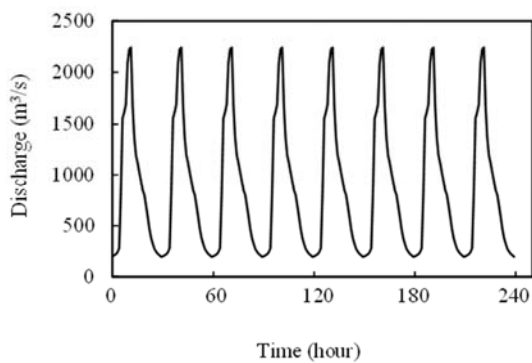


Figure 12. Hydrograph of numerical simulation about channel shape variation.

5.3. Prediction of Topographic Variation

Figure 13 shows the simulation of channel shape variation after 8 times of the flood of July 2012 (The hydrograph is shown in Figure 12). After 8 times of floods, there was sediment accumulation of 3m thick at 18.7km point. Figure 14 shows the cross-sectional morphology of the channel along the dotted line shown in Figure 13 (b). The rate of sediment accumulation become slower as flood repeated.

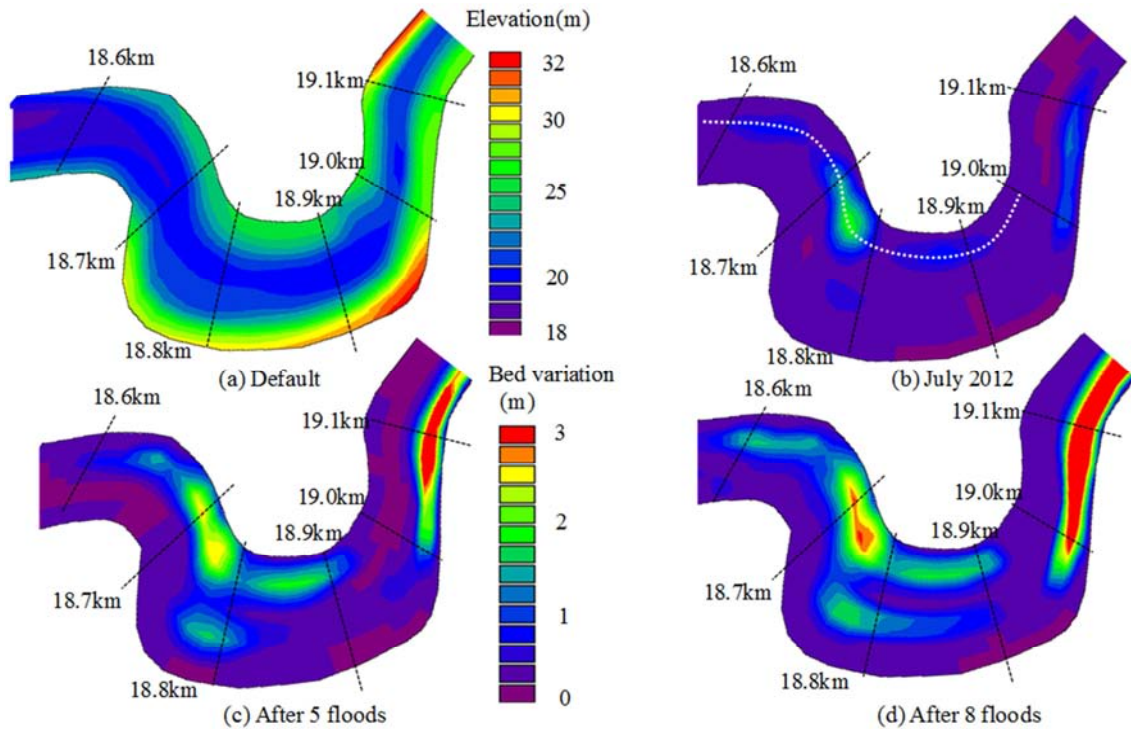


Figure 13. Simulation of channel shape variation after 8 times of the flood of July 2012.

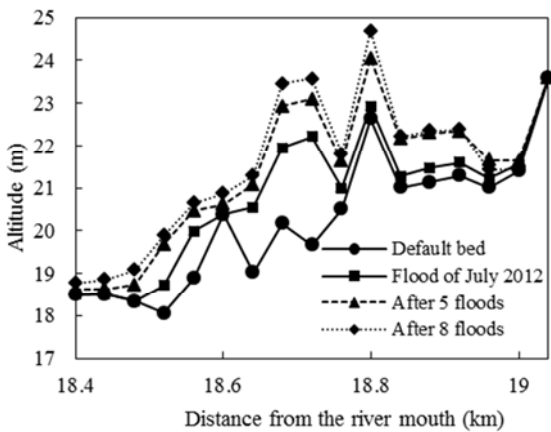


Figure 14. Cross sectional morphology of the channel.

5.4. Effect of Sediment Accumulation on Flood Capacity

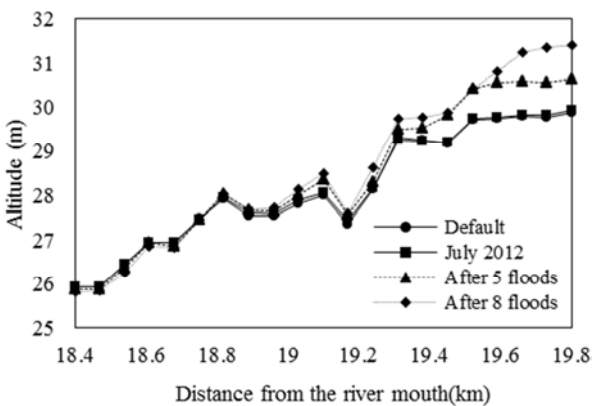


Figure 15. Water level along the center line of the channel.

Figure 15 shows the water level along the center line of the channel. There was little variation from 13.9km point toward the lower reach. On the other hand, the water level increased for 1.5m at the upper reach of the channel after 8 times of floods. This result suggests that sediment accumulation has a negative effect on flood capacity.

6. Conclusion

In this study, the effect of channel variation on the flood capacity was evaluated. The results obtained are as follows.

- (1) Sediment accumulated on the new channel of the Shirakawa River. The thickness of the sediment accumulation was about 3.0m.
- (2) The sediment accumulation caused water level elevation of 1.5m in the upstream area.
- (3) According to the riverbed variation analysis by simulated floods, further accumulation will proceed in the sandbar of the channel of the Shirakawa River, and the flood capacity is expected to be decreasing by further sediment accumulation.

References

- [1] A. Suzuki, M. Fukushima, Y. Yamamoto, and Y. Suwa, "Research on case study about revetment of small and medium-sized river which frequently affected by disaster," *Advances in River Engineering*, Vol. 23, pp. 151-154, 2017.
- [2] Ministry of Land, Infrastructure and Transport Kyushu Regional Development Bureau Kumamoto Office, "Shirakawa water system river maintenance plan", 2013.

- [3] Civil Engineering Association Kyushu Northern Heavy Rain Disaster Investigation Team, "July 2012 Kyushu Northern Heavy Rain Disaster Civil Engineering Study Team Report", 2013.
- [4] H. Yamamoto, T. Yamasaki, M. Yamamoto and h. Kobayashi, "Characteristics of heavy rainfall and flood disaster in kumamoto prefecture on July 12, 2012", Journal of Japan Society for Natural Disaster Science, Vol. 33, No. 2, pp. 83-100, 2014.
- [5] S. Sugio, K. Watanabe, "Research on the change of topographical features and vegetated region on floodplain in river", Annual journal of Hydraulic Engineering, Vol. 48, pp. 985-990, 2004.
- [6] S. Sugio, K. Watanabe, "Analysis on the CHANGE OF VEGETATION LUXURIANCE SITUATIONS on honmura floodplain in the kita river", Annual journal of Hydraulic Engineering, Vol. 49, pp. 1435-1440, 2005.
- [7] S. Sugio, K. Watanabe, Y. Ogawa, S. Morokawa, and R. Hirakawa, "On the change of vegetation on kawasaka floodplain in the kita river", Advances in River Engineering, Vol. 13, pp. 195-200, 2007.
- [8] R. Hirakawa, K. Watanaba and T. Kominami, "Instruction between Topographic Changes and Herbaceous Vegetation of Sand Bar", Journal of applied mechanics, Vol. 68, No. 2, pp. 617-624, 2012.
- [9] T. Uchida, S. Fukuoka, "Bottom velocity computation method by depth integrated model without shallow water assumption", Annual journal of Hydraulic Engineering, Vol. 68, No. 4, pp. 1225-1230, 2012.
- [10] T. Uchida, S. Fukuoka, "A new calculation method for local three-dimensional flows by using the non-hydrostatic depth integrated model (BVC method) with dynamic wall-law for rough bed, Annual journal of Hydraulic Engineering, Vol. 71, No. 2, pp. 43-62, 2015.
- [11] S. Kato, S. Fukuoka, and T. Uchida, "Three-dimensional flows against bank protection works and forces on river banks in the jyoganji river field experiment", Advances in River Engineering, Vol. 23, pp. 155-160, 2017.
- [12] H. Sakamoto, M. Shige-eda, J. Akiyama, M. Shiga, T. Ono, M. Aratake, S. Murakoshi, S. Hirao, T. Iwasa, and Y. Tada, "Examination of appropriate countermeasures at the bifurcation point of the gokasa river based on hydraulic model experiment and quasi 2-d flood flow analysis" Advances in River Engineering, Vol. 23, pp. 465-470, 2017.
- [13] Meyer-Peter and Müller R. "Formulas for bed load transport", Proc. 2nd Congress of IAHR, Stockholm, 1948.